

Effects of Various Post-Treatments of Carbon Nanotube Films for Reliable Field Emission

Jae-Hee Han, Su Hong Lee, Alexander S. Berdinsky, Ji-Beom Yoo, Chong-Yun Park

Center for Nanotubes and Nanostructured Composites,
Department of Materials Engineering, Sungkyunkwan University, 300 Chunchun-Dong, Jangan-Gu, Suwon,
440-746, Korea

Jin Ju Choi

School of Electronics Engineering, Gwangwoon University, 447-1, Wolgye-dong Nowon-Gu, Seoul,
139-701, Korea

Taewon Jung, In Taek Han, Jong Min Kim

Materials and Devices Lab., Samsung Advanced Institute of Technology, P.O.Box111, Suwon, 440-600,
Korea

Abstract

In this report, the FE characteristics of carbon nanotubes (CNTs) treated using both thermal annealing and mechanical coatings on the as-grown CNTs systemically studied. It was found that in the high temperature annealed samples, CNTs were attacked at its root during annealing due to a small amount of oxygen, and were pulled out of the substrate in places after FE measurements because of the contact resistance. However, for the mechanically coated samples both with spin on glass (SOG) and polymethyl methacrylate (PMMA), CNTs were found to be nearly intact after FE measurements and showed reliable FE characteristics over repeatable voltage scan. The reliability of CNTs during FE could be owing to the strong adhesion of CNTs to the substrate both by SOG and PMMA coatings.

1. Introduction

Field emission (FE) of carbon nanotubes (CNTs) has been one of the most promising fields for practical applications of CNTs over a decade [1-3]. Still, however, there are some obstacles such as a low turn-on electric field, current density, current stability and reliability, etc. to make a commercialization of CNTs-based device such as the field emission display. Among those is the reliability of FE rising from the catastrophic degradation of CNTs cathode due to contact resistance [4], resistive heating [5], and bulk properties of CNTs, etc. Here we report the effect of the various post-treatments, such as thermal and mechanical treatments, on the FE characteristics of CNT films for improving the reliability of FE.

2. Experiments

We have grown CNT films directly on the catalyst metal/TiN (200 nm)-coated, polished Ni substrates (thickness~1 mm) by dc plasma-enhanced chemical-vapor deposition (dc-PECVD) method using a gas mixture of C₂H₂ and NH₃. As the catalyst, the mixture of 0.1 g Co acetate [(CH₃CO₂)₂Co] and 0.1 g Fe acetate [(CH₃CO₂)₂Fe] dissolved in 250 ml methanol was spin-coated on

the substrate at 2000 rpm for 30 seconds. Then the substrate was dried at 90 °C for 40 minutes in the air furnace, followed by the CNTs growth was performed by dc-PECVD at 77 W of plasma intensity, 650 °C of temperature, and 3 Torr of working pressure. Detailed processes for the growth of CNTs were described in our previous report [6]. For the thermal annealing treatment, the samples were introduced into the furnace and annealed at temperature ranging from 700 and 1000 °C for 1 hr in N₂ atmosphere. In case of mechanical treatment, the samples were spin-coated either by spin on glass (SOG) or polymethyl methacrylate (PMMA) solutions.

For the analysis of the surface morphology and the crystallinity of the CNTs film, field-emission scanning-electron microscopy (FESEM) and Raman spectroscopy were used. The FE characteristics of CNTs were measured in a vacuum chamber with a parallel diode-type configuration at 3×10^{-6} Torr. The distance between a stainless steel anode and the sample was 200 mm and maintained using a ceramic spacer.

3. Results and Discussion

Figure 1 shows the SEM images before and after FE measurement on the CNTs film grown on a Ni substrate. Many CNTs were locally disappeared after FE compared with as-grown one, which results in decrease in the population density of them. To resolve the failure problem during FE, we made use of two methods; those are thermal and mechanical treatments after growing CNTs.

First, in order to improve the interface properties such as contact resistance and adhesion between the CNTs and TiN-coated substrate, CNTs film was annealed at different high temperatures (700 and 1000 °C) for 1 hr under nitrogen (N₂) atmosphere after synthesis. This annealing treatment was designed to form a stable compound phase (for instance, TiC) between the CNTs and TiN buffer layer at interface attribute to the carbon diffusion into the TiN layer at such temperatures, which probably allows to decrease in contact resistance and increase in adhesion

[7]. Figure 2(a) and (b) show the SEM images of the CNTs annealed at 700 °C before and after FE measurement, respectively. The image of the 700 °C annealed sample before FE measurement was nearly similar to that of the as-grown one (not shown here). After FE measurement, it was found that the longer CNTs with higher field enhancement factors were preferentially broken, which results in leveling off the length of CNTs. For the CNTs annealed at 1000 °C in Fig. 2(c), the average length of CNTs was found to shorten, and some of them seemed to fall down and collapse [see the inset of Fig 2(c)], as compared to the 700 °C annealed one [Fig. 2(a)]. It can be seen that the larger part of the 1000 °C annealed sample was failed after FE measurement as shown in Fig. 2(d), compared with the 700 °C annealed one [Fig. 2(b)]. To examine the annealing effect on the crystallinity of CNTs qualitatively, we used Raman spectroscopy, where the degree of the crystallinity of CNTs can be known by comparing the relative peak intensity ratio of D-band (defect-like band, $\sim 1358 \text{ cm}^{-1}$) and G-band (graphite-like band, $\sim 1582 \text{ cm}^{-1}$) [8,9]. As shown in Fig. 2(e) and (f), the value of $I(D_{peak})/I(G_{peak})$ decreased with annealing temperature, providing an implication of improvement of the crystallinity of CNTs as expected. It was also found that the $I(D_{peak})/I(G_{peak})$ decreased rapidly in the range of 700 to 1000 °C. This corresponds to the apparent structural change of CNTs in that range as mentioned in the previous paragraph. It is well known that the heating of CNTs at high temperature under high vacuum or inert gas atmosphere provide an improvement of the degree of the crystallization of CNTs [8]. However, as seen in Fig. 2(a) and (c), the longer CNTs were removed as the temperature increased from 700 to 1000 °C. The reason for this will be discussed further below.

Let us state the reason for the failure of CNTs after FE measurement. From the results shown in Fig 2(b) and (d), it is speculated that if the voltage drop occurs due to the contact resistance at interface between CNTs and substrate during FE, CNTs will be damaged and removed. There have been a lot of reports for the singlewall CNT-based transistor structures on contact resistance (R_c) between CNT and metal electrodes, which significantly affects the devices performance [10-11]. Singlewall CNTs are one-dimensional quantum systems and the two-terminal conductance is given by Landauer-Buttiker formalism as: $G_c = N \cdot e^2/h \cdot T$, where N is the number of conduction channels in parallel, e the electron charge, and T the transmission coefficient [12]. If the contact is perfect ($T = 1$) and the CNT is scattering free, charge carriers can move through the nanotube ballistically, we have the total resistance of a single-walled CNT contacted by metal leads on both ends is the sum of these two contributions, $R_t = R_c = h/4e^2 \sim 6.5 \text{ k} = R_0$. This lower limit of resistance arises from the mismatch of the number of conduction channels in singlewall CNT and the macroscopic metal leads. Bonard *et al.* attributed the failure of individual multiwall CNTs during FE to mechanical failure of the contact at low applied fields, and to resistive heating at high emitted currents [4]. From those reports, it can be conjectured that when CNT contacts with a metal electrode, there must exist a certain value of contact resistance, and it could be still larger if the system has some electron scattering sources such as a crystal imperfection of CNT and rough touching of CNT and the metal lead at interface. During FE measurement, a voltage drop should occur at the interfaces between CNTs and substrate with such contact resistance depending on their own configurations. This leads to making a mechanical stress and/or the electrically-driven resistive Joule heating at the CNTs root, giving rise to the rupture and removing

of CNTs from the substrate in the event as show in Fig. 2(b) and (d).

In order to avoid the failure of CNTs during FE, we alternatively used the mechanical adhesive coating on the as-grown CNTs film, for which either 33 wt% SOG dissolved in terpineol or 10 wt% PMMA in DMF were employed as coating agents. Figure 3(a) and (c) shows the SEM images of the resulting CNTs films, which were coated with SOG and PMMA and subsequently wet-etched such that CNTs were barely exposed by diluted hydrofluoric acid and acetone, respectively. One can see that most of the CNTs were coated and bundled in both case, as compared with Fig. 2(a). After FE measurements, it seems that the majority of CNTs was nearly intact, which implies that both mechanical coatings are very useful methods for anchoring CNTs to the substrate during FE.

The multiple scans plots of FE current density (J) versus applied electric field (E) characteristics for the CNTs films that were post-treated using both thermal and mechanical methods are given in Fig. 4. The turn-on electric field, E_{to} , is defined as the onset electric field in the Fowler-Nordheim (FN) plot (shown in the all insets of Fig 4). For the 1st FE scan [Fig 4(a)], the E_{to} for the as-grown CNTs sample (denoted by crosses) was the lowest value of 1.75 V/ μm , and showed the best FE property. However, FE behaviors were significantly deteriorated over repetition of voltage scans, and finally no detectable FE current was measured as shown in Fig. 4, reminding of the failure of CNTs seen in Fig. 1. In case of the CNTs sample annealed at high temperatures, the FE properties of the 700 °C annealed sample (denoted by empty circles) were always superior to those of the 1000 °C annealed one (denoted by empty up -triangles) over whole scans. In additions, it was found that the maximum current of the latter decreased more rapidly than that of the former. This is inconsistent with the results from Raman spectra shown in Fig. 2(e) and (f), where the crystallinity of CNTs was better with temperature, probably leading to the decrease in CNTs resistance. If so, the FE of the latter should be expected to show better characteristics than that of the former. This contradiction could be briefly elucidated as follows: (i) one possible reason is the oxidation of the longer CNTs with higher probability of meeting oxygen, which is contained at a small amount in the furnace likely enough, in the CNT forest. (ii) the other is the preferential oxidation of the CNTs at the root (i.e., interface between CNT and TiN buffer layer) because of likely more defects therein. The latter is more plausible since the structural defects in the root of CNTs would have a larger probability than in the tip or body. Therefore we put forward a scenario that when the root part of CNTs is damaged due to the oxygen contamination during annealing in the furnace, the contact resistance increases and/or the adhesion is worse, which causes to the failure of CNTs during FE and thus the decrease in FE current at a given electric field. The examination of how amount of oxygen exists should be needed.

For the CNTs coated either by SOG or PMMA, there was no detectable current initially in the 1st scan as shown in Fig. 4(a), because the whole outmost shells of CNTs were coated with such agents so that no emission sites exist at the beginning. Then the FE current increased suddenly with voltage possibly due to the vaporizing of the agents from the CNTs wall under higher electric fields. After that, the emission currents were reliably measured over repeatable voltage scans attributing to the strong mechanical adhesion of CNTs to the substrate. Until now, since the etching conditions for SOG and PMMA have not been established, we

cannot conclude which one is a more suitable adhesion agent for CNTs.

4. Conclusion

We systematically studied the FE characteristics of CNTs post-treated using both thermal annealing and mechanical coatings after growing CNTs. It was found that in the high temperature annealed samples, CNTs were somewhat damaged during annealing, and the failure of CNTs occurred due to the contact resistance after the FE measurements. However, in the case of the mechanically coated samples both with SOG and PMMA, CNTs were found to be nearly intact after FE measurements and showed nearly the identical FE behaviors reliably over repeatable voltage scans. The reliability of CNTs during FE could be attributed to the strong adhesion of CNTs to the substrate both by SOG and PMMA coatings.

5. Figures/Captions

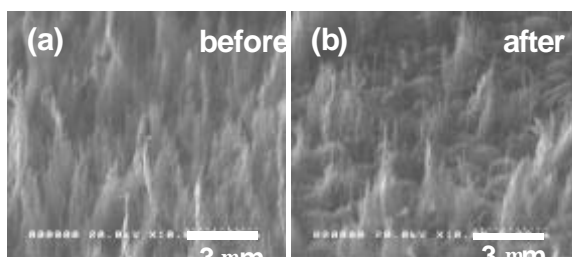


Fig. 1. The SEM images before and after FE measurement on the CNTs film grown on a Ni substrate.

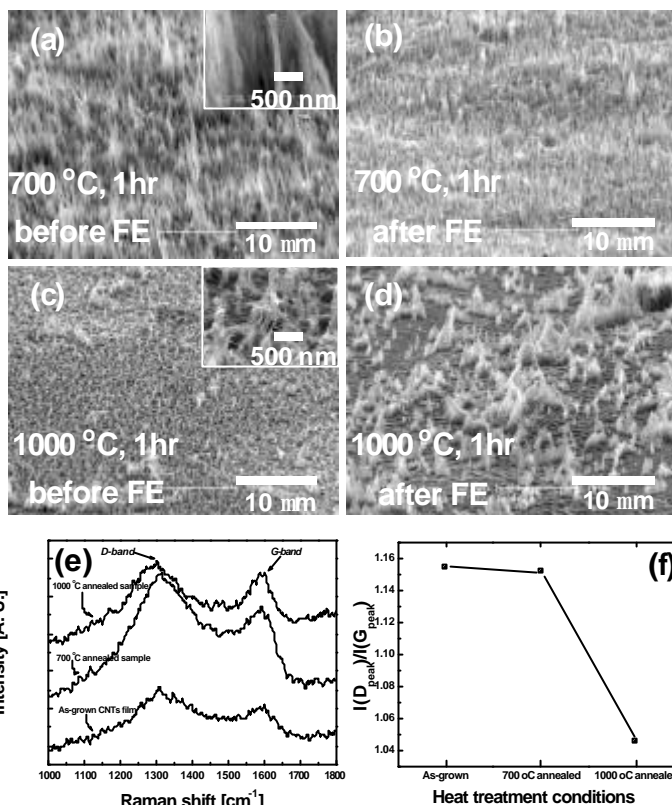


Fig. 2. The SEM images of the CNTs annealed at 700 °C (a) before and (b) after FE measurement, and of the CNTs annealed at 1000 °C (c) before and (d) after FE, in sequence. (e) Raman spectra for the as-grown CNTs, the 700 and 1000 °C annealed samples. (f) The relative peak intensity ratio of D-band and G-band [$I(D_{peak})/I(G_{peak})$] for three samples.

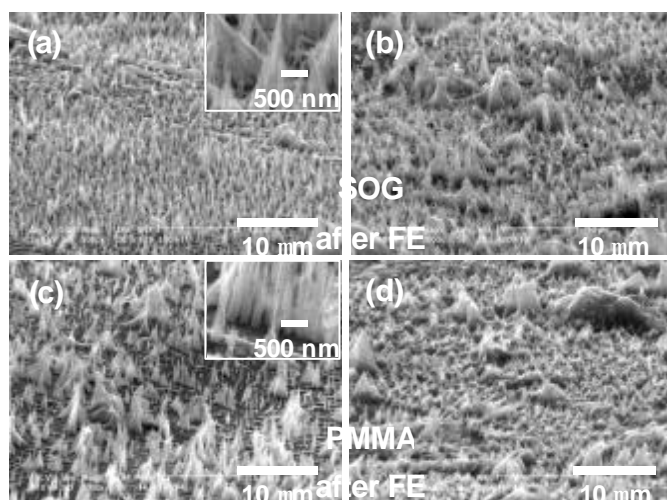


Fig. 3. The SEM images of the CNTs films, which were first coated with SOG and PMMA and subsequently wet-etched by diluted HF acid and acetone, respectively.

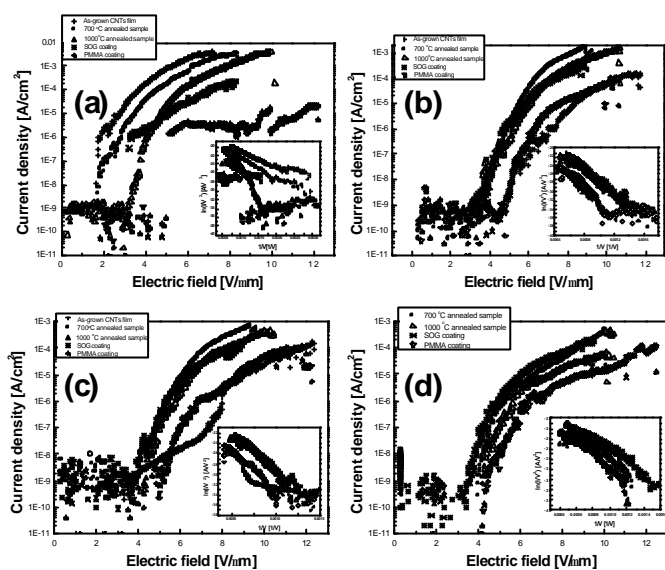


Fig. 4. (a-d) The sequential multiple scans plots of FE current density (J) versus applied electric field (E) characteristics for the CNTs films that were post-treated using both thermal and mechanical methods.

6. References

- [1] W. A. de Heer, A. Chatelain, and D. Ugarte, *Science* **270**, 1179 (1995).
- [2] W. B. Choi, D. S. Chung, J. H. Kang, H. Y. Kim, Y. W. Jin, I. T. Han, Y. H. Lee, J. E. Jung, N. S. Lee, G. S. Park, and J. M. Kim, *Appl. Phys. Lett.* **75**, 3129 (1999).
- [3] P. G. Collins, M. Hersam, M. Arnold, R. Martel, and Ph. Avouris, *Phys. Rev. Lett.* **86**, 3128 (2001).
- [4] J. -M. Bonard, C. Klinke, K. A. Dean, and B. F. Coll, *Phys. Rev. B* **67**, 115406 (2003).
- [5] K. A. Dean, T. P. Burgin, and B. R. Chalamala, *Appl. Phys. Lett.* **79**, 1873 (2001).
- [6] J. H. Han, J. B. Yoo, C. Y. Park, H. J. Kim, G. S. Park, M. H. Yang, I. T. Han, N. S. Lee, and J. M. Kim, *J. Appl. Phys.* **91**, 483 (2002).
- [7] Y. Zhang, T. Ichihashi, E. Landree, F. Nihey, S. Iijima, *Science* **285**, 1719 (1999).
- [8] T. C. Chieu, M. S. Dresselhaus, M. Endo, *Phys. Rev. B* **26**, 5867 (1982).
- [9] M. Chhowalla, K. B. K. Teo, C. Ducati, N. L. Rupesinghe, G. A. J. Amaratunga, A. C. Ferrari, D. Roy, J. Robertson, and W. I. Milne, *J. Appl. Phys.* **90**, 5308 (2001).
- [10] S. J. Tans, A. R. M. Verschueren, and C. Dekker, *Nature* **393**, 49 (1998).
- [11] R. Martel, V. Derycke, C. Lavoie, J. Appenzeller, K.K. Chan, J. Tersoff, and Ph. Avouris, *Phys. Rev. Lett.* **87**, 256805 (2001).
- [12] S. Datta, *Electronic Transport in Mesoscopic Systems*, Cambridge, U.K.: Cambridge Univ. Press (1995).